

NASA Technical Paper 1191

LOAN COPY: RETURN TO
AFWL TECHNICAL LIBRARY
KIRTLAND AFB, N. M.

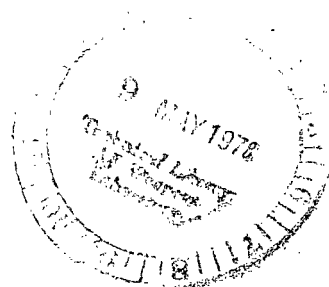


Friction and Metal Transfer for Single-Crystal Silicon Carbide in Contact With Various Metals in Vacuum

Kazuhisa Miyoshi and Donald H. Buckley

APRIL 1978

NASA





NASA Technical Paper 1191

Friction and Metal Transfer
for Single-Crystal Silicon
Carbide in Contact With
Various Metals in Vacuum

Kazuhisa Miyoshi
Kanazawa University
Kanazawa, Japan

Donald H. Buckley
Lewis Research Center
Cleveland, Ohio



National Aeronautics
and Space Administration

**Scientific and Technical
Information Office**

1978

FRICITION AND METAL TRANSFER FOR SINGLE-CRYSTAL SILICON CARBIDE IN CONTACT WITH VARIOUS METALS IN VACUUM

by Kazuhisa Miyoshi* and Donald H. Buckley

Lewis Research Center

SUMMARY

An investigation was conducted to examine the friction behavior of single-crystal silicon carbide in contact with various metals and the nature of metal transfer to silicon carbide. Sliding friction experiments were conducted with silicon carbide in sliding contact with transition metals (tungsten, iron, rhodium, nickel, titanium, and cobalt), copper, and aluminum. All experiments were conducted with loads of 5 to 50 grams, at a sliding velocity of 3 millimeters per minute, in a vacuum of 10^{-8} pascal and at 25°C on the (0001) basal plane in the $\langle 10\bar{1}0 \rangle$ directions.

The results of the investigation indicate that the coefficient of friction for a silicon carbide in contact with various metals is related to the d bond character and relative chemical activity of the metal. The more active the metal, the higher the coefficient of friction. All the metals examined transferred to the surface of silicon carbide in sliding. The chemical activity of metal to silicon and carbon and shear modulus of metal may play important roles in metal-transfer and the form of the wear debris. The less active and more resistant to shear the metal is, with the exception of rhodium and tungsten, the less transfer to silicon carbide. Aluminum and titanium, having much stronger chemical affinity and less resistance to shear than the other metals, exhibited the greatest amount of transfer. Rhodium and tungsten have the greatest resistance to shear, and the character of the wear particles for these metals is different from that observed for the other metals.

INTRODUCTION

Silicon carbide has great usefulness in high-hardness or high-temperature applica-

*Assistant Professor of Precision Engineering, Kanazawa University, Kanazawa, Japan; National Research Council - National Aeronautics and Space Administration Research Associate.

tions such as a stable high-temperature semiconductor and a turbine ceramic seal system, and as an abrasive for grinding. The present authors have conducted experimental work to determine the tribophysical properties of single-crystal silicon carbide. This work has included a determination of (a) the friction and wear behavior of silicon carbide in contact with itself and titanium (refs. 1 and 2), (b) the friction, deformation, and fracture behavior of silicon carbide in contact with diamond, and (c) the influence of the crystallographic orientation of silicon carbide on its friction and deformation (refs. 3 and 4).

The present investigation was conducted to examine the friction behavior of single-crystal silicon carbide in contact with various metals and to examine the nature of metal-transfer to silicon carbide. All experiments were conducted with loads of 5 to 50 grams, at a sliding velocity of 3 millimeters per minute, in a vacuum of 10^{-8} pascal, at 25° C, and on the (0001) basal plane in the $\langle 10\bar{1}0 \rangle$ directions. The radius of the metal pin specimens was 0.79 millimeter.

MATERIALS

The single-crystal silicon carbide platelets used in these experiments were a 99.9-percent pure compound of silicon and carbon (table I). The silicon carbide has a hexagonal-close-packed crystal structure. The C direction was perpendicular to the sliding interface, with the basal plane therefore parallel to the interface. The Knoop hardness is 2954 ± 27 in the $\langle 10\bar{1}0 \rangle$ and 2917 ± 10 in the $\langle 11\bar{2}0 \rangle$ directions on the basal plane of silicon carbide (ref. 5).

The metals were all polycrystalline. The titanium was 99.97 percent pure, the copper was 99.999 percent pure, and all the other metals were 99.99 percent pure. Table I shows the crystalline, physical, and chemical properties of single-crystal silicon carbide and metal specimens.

APPARATUS

The apparatus used in the investigation was mounted in an ultra-high vacuum system. The apparatus is capable of measuring adhesion, load, and friction. The vacuum system also contained tools for surface analysis, an Auger emission spectrometer (AES), and a LEED (low-energy electron diffraction) system. The mechanism used for measuring adhesion, load, and friction is shown schematically in figure 1. A gimbal-mounted beam is projected into the vacuum system. The beam contains two flats machined normal to each other with strain gages mounted thereon. The metal pin is mounted on the end of the beam. As a load is applied by moving the beam normal to the

disk, it is measured by the strain gage. The vertical sliding motion of the pin along the disk surface is accomplished through a motorized gimbal assembly. Under an applied load the friction force is measured during vertical translation by the strain gage mounted normal to that used to measure load. This feature was used to examine the coefficient of friction at various loads, as shown in figure 1. Multiple wear tracks could be generated on the disk surface by the translating motion of the beam containing the pin.

EXPERIMENTAL PROCEDURE

The disk flat (silicon carbide) and metal pin specimens were polished with a diamond powder (particle diameter, $3\text{ }\mu\text{m}$) and with an aluminum oxide (Al_2O_3) powder ($1\text{ }\mu\text{m}$). The radius of the pins was 0.79 millimeter. The disk and pin surfaces were rinsed with 200-proof ethyl alcohol.

The specimens were placed in the vacuum chamber, and the system was evacuated and subsequently baked out to obtain a pressure of 1.33×10^{-8} pascal (10^{-10} torr). When this pressure was obtained, argon gas was bled back into the vacuum chamber to a pressure of 1.3 pascals. A 1000-volt-direct-current potential was applied, and the specimens (both disk and rider) were argon sputter bombarded for 30 minutes. One hour after the sputtering operation was completed the vacuum chamber was reevacuated, and AES spectra of the disk surface were obtained to determine the degree of surface cleanliness. When the desired degree of cleanliness of disk was achieved, friction experiments were conducted (refs. 1 and 2).

Loads of 5 to 50 grams were applied to the pin-disk contact by deflecting the beam of figure 1. Both load and friction force were continuously monitored during a friction experiment. Sliding velocity was 3 millimeters per minute, with a total sliding distance of 2.5 millimeters. All friction experiments in vacuum were conducted with the system evacuated to a pressure of 10^{-8} pascal.

RESULTS AND DISCUSSION

Effect of Metal Activity on Friction

The relative chemical activity of the transition metals (metals with partially filled d shells) as a group can be ascertained from their percent d bond character after Pauling (ref. 6). The strength of adhesion and coefficient of friction of the transition metals in contact with metal have been shown to be related to this property of the metals (ref. 7). The greater the percent d bond character, the less active the metal and

the less the coefficient of friction.

It is of interest to determine whether the foregoing concept carries over into the interactions of ceramic-to-metal interfaces. The authors have shown that the chemical activity of a metal plays a role in the adhesion and friction of manganese-zinc ferrite-to-transition metals (ref. 8).

The coefficients of friction for a number of transition metals in contact with single-crystal silicon carbide are presented in figure 2 as a function of load and in figure 3 as a function of the δ bond character of the transition metal.

Examination of figure 2 indicates no significant change in coefficient of friction with load. The friction traces were primarily characterized by marked stick-slip behavior over the entire load range, as shown in figures 5 and 8 in a later section. This type of friction is expected where strong adhesion occurs at the interface. Note that the average coefficient of friction in figures 2 and 3 was calculated from maximum-peak-heights in the friction trace resulting from a single-pass sliding of metal rider.

The data of figure 3 indicate a decrease in friction with an increase in δ character of the metallic bond. There appears to be very good agreement between friction and chemical activity of the transition metals.

Aluminum and copper both have a chemical affinity for silicon and carbon. Their affinity for silicon is not as great as for carbon (ref. 9). However, copper is less chemically active with respect to both silicon and carbon, indicating that it does not have as strong a chemical affinity or tendency to bond to these elements as does aluminum.

Data were obtained for aluminum and copper sliding on single-crystal silicon carbide. Coefficients of friction as a function of load are presented in figure 4. Examination of figure 4 indicates no significant change in coefficient of friction with load, a behavior analogous to that observed with silicon carbide in contact with transition metals (fig. 2) and silicon carbide in contact with itself (ref. 1). The coefficient of friction of aluminum is approximately 0.6. It is almost the same as that for silicon carbide in sliding contact with the more chemically active titanium and with silicon carbide itself (see fig. 4). It is, however, greater than that for copper in contact with silicon carbide (where the coefficient of friction is approximately 0.4). Hence, with the chemically more active metal aluminum, higher friction is observed. In figure 4 the average coefficient of friction was calculated from maximum-peak-heights in the friction trace resulting from a single-pass sliding of rider.

Thus, the chemical activity or inactivity of a metal, as mentioned, plays a role in adhesion and friction of single-crystal silicon carbide contacting metals.

Transfer of Metals Sliding on Silicon Carbide

All of the single-crystal silicon carbide surfaces contacted by the metals in table I

contained the metallic elements on their surfaces, indicating transfer of the metal to silicon carbide. This occurred with a single pass of the metal rider.

After the single-pass experiments, multipass experiments were conducted to establish transfer of metal. The friction traces resulting from multiple passes are characterized by stick-slip behavior (fig. 5). With the chemically more active titanium the friction traces have a larger amplitude and period of wave. When repeated passes of the metal riders are made over the same single-crystal silicon carbide surface, the coefficient of friction, calculated from maximum peak-heights in friction trace, generally decreases with number of passes to an equilibrium value. This decrease seems to depend on the nature of the transfer of the metals, as indicated by the data of figure 6. The fluctuating behavior of the coefficient of friction also depends on the nature of the transfer of the metals. In contrast, when repeated passes of the silicon carbide rider were made on silicon carbide, the coefficient of friction was generally constant (fig. 6(c)). The type of metal transfer to silicon carbide was generally governed for the four groups of metals by two factors: (1) chemical affinity of the metal for silicon carbide and (2) resistance to shear of the metal, that is, shear modulus.

Aluminum and titanium. - Aluminum and titanium, having much stronger chemical affinity for silicon and carbon (ref. 7) than the other metals, exhibited considerably higher friction. However, they have the least resistance to shear as shown in table I. Sliding of these metals on silicon carbide results in a large amount of transfer of them to silicon carbide.

Figure 7 presents scanning electron micrographs and an X-ray map of a wear track generated by a single pass of the aluminum rider. It becomes obvious from figure 7 that a large amount of aluminum transfers to the silicon carbide in a single pass of the rider. In figure 7(a) the light area of the figure, where a lot of aluminum transfer is evident, was the contact area before sliding of the rider. It is the area where the surfaces of metal and silicon carbide were sticking one to the other, as schematically shown in figure 8; that is, in this area both the loading and tangential force were applied to the specimens, but no sliding had occurred. The top of figure 7(a) is the area where less aluminum transfer is evident after sliding of rider; the surfaces of metal and silicon carbide were in a rapid slip. (See the slip schematic of fig. 8(a).) Note that, in an X-ray energy dispersive analysis for aluminum on the silicon carbide surface shown in figure 7(b), the concentrations of white spots correspond to those locations in figure 7(a) where copious amounts of aluminum transferred. Thus, fracture of cohesive bonds in aluminum occurs in sliding, and the presence of the large amounts of aluminum transfer is in the sticking area, where strong adhesion occurs at the interface. Figure 7(c) illustrates the two types of aluminum wear debris generated by the fracture of cohesive bonds of aluminum: One type is characterized as being cylindrical particles, where the direction of the cylinder is perpendicular to the sliding direction as shown in figure 7(c). The other is a thin film which is streaky and perpendicular to the sliding direction.

After the examination of a wear track generated by a single pass of the rider, a wear track by multipasses of aluminum rider was examined. Figure 9 presents a scanning electron micrograph and an aluminum K_{α} X-ray map of the point of beginning of a wear track on the silicon carbide, generated by 10 passes of the aluminum rider over the same surface. It is obvious from figure 9 that the aluminum transfer is much more than that in the single pass of the aluminum rider shown in figure 7. Further, figure 9 reveals that the multilayer film structure of aluminum transfer was produced by repeated contacting and sliding, as schematically shown in figure 8(b). The multilayer film structure is due to the piling up of aluminum wear debris.

Some other scanning electron micrographs of aluminum transfer to silicon carbide during multipass sliding are shown in figure 10. Figure 10 reveals evidence for four types of wear debris: (1) a very thin transfer film in the entire contact area, (2) multilayer transfer films, (3) very small particles (submicrometer in size), and (4) piled-up particles (several micrometers in size). In addition to the four types of aluminum wear debris or transfer, cylindrical particles (not piled up) shown in figure 7, were detected on the silicon carbide surface (see table II).

Examination of wear tracks on the silicon carbide after single-pass sliding with titanium revealed evidence of both very thin transfer films and lump particles of titanium transferred to the silicon carbide (ref. 2). On the other hand, examination of the silicon carbide surface after multipass sliding with titanium indicates the presence of very thin transfer films, multilayer transfer films, very small particles, and pile up of particles, as indicated in figure 11. Thus, the wear debris of titanium transferred to the silicon carbide is very similar to that observed with aluminum (see table II).

Nickel, copper, and cobalt. - Nickel, copper, and cobalt have less chemical affinity for silicon and carbon and greater resistance to shear than aluminum and titanium (figs. 3 and 4 and table I). Cobalt has a hexagonal crystal structure and with repeated passes over the surface crystallographic texturing would be expected to occur with a corresponding reduction in friction from that observed for the cubic metals nickel and copper.

Figures 12 to 14 are scanning electron micrographs of wear tracks on the silicon carbide surface generated by 10 passes of the riders of these metals over the same silicon carbide surfaces. The figures reveal very thin transfer films, very small particles, and piled-up particles. Nickel produces more transfer of thin films than does copper and cobalt. This appears to be related to the higher coefficient of friction than was observed for copper and cobalt. Note that the average coefficient of friction of nickel was 0.48, of copper 0.40, and of cobalt 0.42. The amount of transfer for nickel, copper, and cobalt to silicon carbide is, however, less than was observed with aluminum and titanium.

Iron. - Iron seems to have almost the same chemical affinity for silicon and carbon as nickel and has greater resistance to shear than it. Figure 15, scanning electron

micrographs of a wear track on the silicon carbide surface generated by 10 passes of the rider, reveals evidence of very small particles and piled-up particles. There is very little evidence for a thin transfer film on the wear track. This is apparently related to the greater resistance to shear of iron than of nickel or copper.

Tungsten and rhodium. - Tungsten and rhodium have the least chemical affinity for silicon and carbon and greatest resistance to shear of all metals in table I. Figure 16 shows scanning electron micrographs of wear tracks on the silicon carbide surfaces generated by a single pass and 10 passes of a tungsten rider. It is obvious that large lumps (several micrometers in size) and very small wear particles (submicrometer size) of tungsten transfer to silicon carbide. Figure 17, scanning electron micrographs of a wear track on the silicon carbide surface generated by 10 passes of a rhodium rider, also reveals large lumps and very small wear particles. As indicated in figure 17, some lump particles were deformed plastically during multipasses sliding.

Tungsten and rhodium can be characterized as producing and transferring lumps of wear particles to silicon carbide as a result of sliding. This may be due to the greater shear moduli of tungsten and rhodium.

Comparison of Metal Transfer

Table II summarizes metal transfer to single-crystal silicon carbide observed after multiple passes of a metal rider over the same silicon carbide (0001) surface. As already mentioned, the chemical affinity of the metal to silicon and carbon and the shear modulus of the metal may play important roles in metal transfer and the form of wear debris generated. Generally, metals farther to the right in table II have less chemical activity for silicon and carbon, lower coefficients of friction, and greater resistance to shear. Furthermore, the metals, except tungsten and rhodium farther to the right in table II, transfer less to silicon carbide. Tungsten and rhodium have the greatest resistance to shear and produce lump wear particles, which are quite different from the wear debris observed for other metals.

CONCLUSIONS

As a result of sliding friction experiments conducted with single-crystal silicon carbide in sliding contact with various metals, the following conclusion are drawn:

1. The coefficient of friction for silicon carbide in contact with various metals is related to the relative chemical activity of those metals. The more active the metal, the higher the coefficient of friction. For the transition metal friction is related to the d bond character of the metal.

2. All the metals examined transferred to the surfaces of silicon carbide in sliding.
3. The chemical activity of metal to silicon and carbon and shear modulus of metal may play important roles in metal-transfer and the form of the wear debris. The less active and more shear resistant the transition metal (except tungsten and rhodium), the less transfer to silicon carbide.
4. Aluminum and titanium, having much stronger chemical affinity and less resistance to shear than the other metals, exhibited the greatest amount of transfer.
5. Tungsten and rhodium have the greatest resistance to shear, and they produce and transfer lump wear particles.

Lewis Research Center,
National Aeronautics and Space Administration,
Cleveland, Ohio, November 17, 1977,
506-16.

REFERENCES

1. Miyoshi, K.; and Buckley, D. H.: Friction and Fracture of Single-Crystal Silicon Carbide in Contact with Itself and Titanium. ASLE Trans.
2. Miyoshi, Kazuhisa; and Buckley, Donald H.: Friction and Wear Behavior of Single-Crystal Silicon Carbide in Contact with Titanium. NASA TP-1035, 1977.
3. Miyoshi, Kazuhisa; and Buckley, Donald H.: Friction and Deformation Behavior of Single-Crystal Silicon Carbide. NASA TP-1053, 1977.
4. Miyoshi, Kazuhisa; and Buckley, Donald H.: Friction, Deformation and Fracture of Single-Crystal Silicon Carbide. NASA TM-73705, 1977.
5. Shaffer, Peter T. B.: Effect of Crystal Orientation on Hardness of Silicon Carbide. J. Am. Ceram. Soc., vol. 47, no. 9, Sept. 1964, p. 466.
6. Pauling, L.: A Resonating-Valence-Bond Theory of Metals and Intermetallic Compounds. Proc. Roy. Soc., Ser. A, vol. 196, no. 1046, 7 Apr. 1949, pp. 343-362.
7. Buckley, Donald H.: The Metal-to-Metal Interface and its Effect on Adhesion and Friction. J. Colloid Interface Sci., vol. 58, no. 1, Jan. 1977, pp. 36-53.
8. Miyoshi, K.; and Buckley, D. H.: Friction and Wear of Single-Crystal and Polycrystalline Manganese-Zinc Ferrite in Contact with Various Metals. NASA TP-1059, 1977.

9. Brewer, L., et al.: Thermodynamic and Physical Properties of Nitrides, Carbides, Sulfides, Silicides, and Phosphides. The Chemistry and Metallurgy of Miscellaneous Materials: Thermodynamics, Laurence L. Quill, ed., McGraw-Hill Book Co., Inc., 1950, pp. 40-59.
10. Taylor, A.; and Laidler, D. S.: The Formation and Crystal Structure of Silicon Carbide. Brit. J. Appl. Phys., vol. 1, 1950, pp. 174-181.
11. Drowart, J.; and DeMaria, G.: Thermodynamic Study of the Binary System Carbon-Silicon Using a Mass Spectrometer. Silicon Carbide: A High Temperature Semiconductor, J. R. O'Connor and J. Smiltens, eds., Pergamon Press, 1960, pp. 16-23.
12. Carnahan, R. D.: Elastic Properties of Silicon Carbide. J. Am. Ceram. Soc., vol. 51, no. 4, Apr. 1968, pp. 223-224.
13. Barrett, Charles Sanborn: Structure of Metals, Crystallographic Methods, Principles, and Data. McGraw-Hill Book Co., Inc., 1943, pp. 552-554.
14. Gschneidner, Karl A., Jr.: Physical Properties and Interrelationships of Metallic and Semimetallic Elements. Solid State Physics, vol. 16, Frederick Seitz and David Turnbull, eds., Academic Press, 1965, pp. 275-426.
15. Glasstone, Samuel: Thermodynamics for Chemists. D. Van Nostrand Reinhold Co., Inc. 1947, p. 479.
16. Pierce, Willis Conway; and Haenisch, Edward Lauth: Quantitative Analysis. Third ed. John Wiley & Sons, Inc., 1948, pp. 270-271.

TABLE I. - CRYSTALLINE, PHYSICAL, AND CHEMICAL PROPERTIES OF SINGLE-CRYSTAL SILICON CARBIDE AND METAL SPECIMENS

| Material | Purity, percent | Crystal structure at 25° C | Lattice constant, Å | | | Cohesive energy | | Shear modulus | | Amount of d character, percent | Standard oxidation- reduction potentials (elec- tromotive force) |
|-----------------------|--------------------|-------------------------------|---------------------|---------|--------|---|----------------------------------|---|------|--------------------------------------|--|
| | | | a | c | a/c | 10^6 $\frac{\text{kcal}}{\text{g-atom}}$ | $\frac{\text{J}}{\text{g-atom}}$ | 10^6 $\frac{\text{kg}}{\text{cm}^2}$ | GPa | | |
| SiC ^b | 99.9 | Hexagonal close-packed | 3.0817 | 15.1183 | 4.9058 | ^c 125±3 | ^c 523 | 2.04 | 200 | ---- | ----- |
| Tungsten ^d | 99.99 | Body-centered cubic | 3.1586 | ----- | ----- | 199.7 | 835.5 | 1.56 | 15.3 | 43 | ----- |
| Iron ^d | ↓ | Body-centered cubic | 2.8640 | ----- | ----- | 99.4 | 416 | .831 | 8.15 | 39.7 | Fe → Fe ⁺⁺ + 2e + 0.44 eV |
| Rhodium ^d | | Face-centered cubic | 3.7956 | ----- | ----- | 133.0 | 556.5 | 1.50 | 14.7 | 50 | ----- |
| Nickel ^d | | Face-centered cubic | 3.5169 | ----- | ----- | 102.3 | 428.0 | .765 | 7.50 | 40 | Ni → Ni ⁺⁺ + 2e + 0.25 eV |
| Titanium ^d | 99.97 | Hexagonal close-packed | 2.953 | 4.729 | 1.587 | 112.2 | 469.4 | .401 | 3.93 | 27 | Ti → Ti ⁺⁺ + 2e + 1.75 eV |
| Cobalt ^d | 99.99 | Hexagonal close-packed | 2.507 | 4.072 | 1.624 | 101.7 | 425.5 | .779 | 7.64 | 39.5 | Co → Co ⁺⁺ + 2e + 0.28 eV |
| Copper ^d | 99.999 | Face-centered cubic | 3.6080 | ----- | ----- | 80.8 | 338 | .460 | 4.51 | ---- | Cu → Cu ⁺⁺ + 2e - 0.34 eV |
| Aluminum ^d | 99.99 | Face-centered cubic | 4.0414 | ----- | ----- | 76.9 | 322 | .271 | 2.66 | ---- | Al → Al ⁺⁺⁺ + 3e + 1.67 eV |

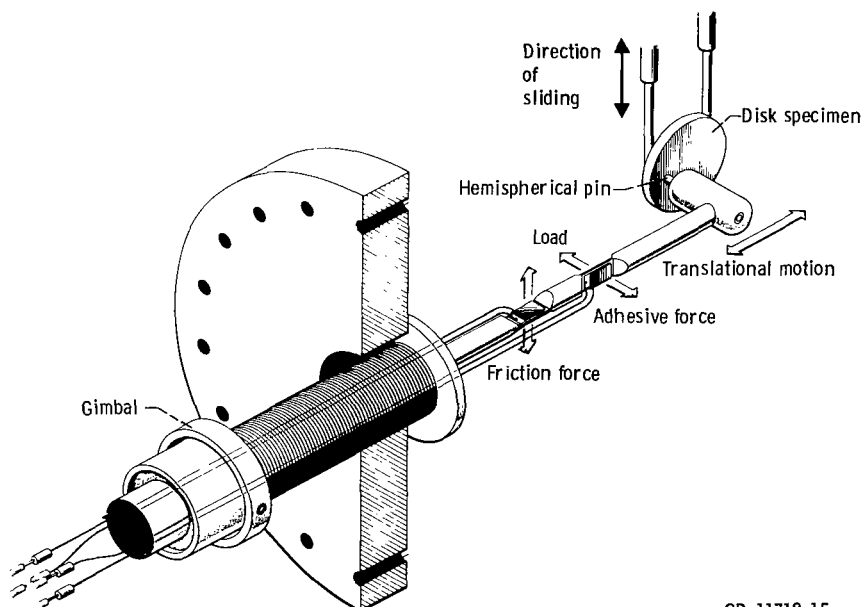
^aSource of data: manufacturer's analysis.^bSources of data: Lattice constants, ref. 10; cohesive energy, ref. 11; shear modulus, ref. 12.^cHeat of formation of gaseous silicon and graphite from hexagonal silicon carbide.^dSources of data: Crystal structure and lattice constants, ref. 13; cohesive energy and shear modulus, ref. 14; amount of d character, ref. 6; standard oxidation-reduction potentials, refs. 15 and 16.

TABLE II. - METAL TRANSFER TO SINGLE-CRYSTAL SILICON

CARBIDE (0001) SURFACE AS A RESULT OF MULTIPLE PASSES

[Transferred after 10 passes sliding, +; not transferred after 10 passes sliding, -; transferred after single pass sliding (+).]

| Form of metal transfer | Metals | | | | | | | |
|--|--------|-----|----|----|----|----|----|---|
| | Al | Ti | Cu | Ni | Co | Fe | Rh | W |
| Very small particle (submicrometer size) | + | + | + | + | + | + | + | + |
| Piled-up particle (several micrometers in size) | + | + | + | + | + | + | - | - |
| Streak thin film | + | + | + | + | + | - | - | - |
| Multilayer film structure (piled-up) | + | + | - | - | - | - | - | - |
| Lumps (several micrometers in size) | (+) | (+) | - | - | - | - | + | + |



CD-11718-15

Figure 1. - High-vacuum friction and wear apparatus.

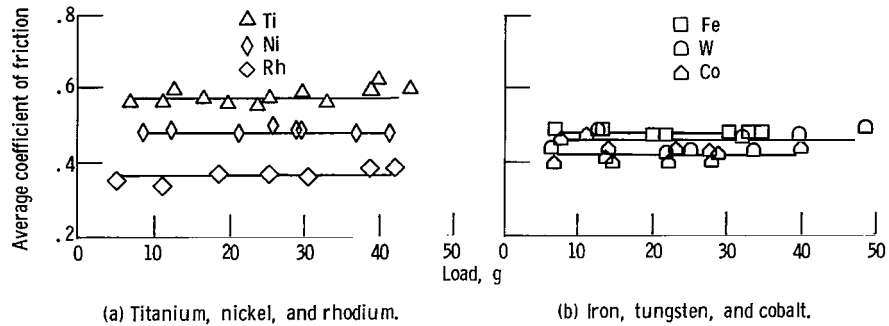


Figure 2. - Average coefficient of friction, calculated from maximum-peak-heights in friction trace, as function of load for various transition metals sliding on single-crystal silicon carbide (0001) surface. Single pass of metal rider; sliding direction, $\langle 10\bar{1}0 \rangle$; sliding velocity, 3 millimeters per minute; temperature, 25°C ; vacuum pressure, 10^{-8} pascal.

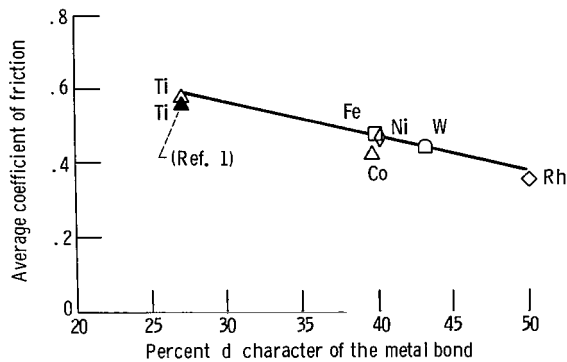


Figure 3. - Average coefficients of friction for loads from 5 to 50 grams as function of percent of metal d bond character for single-crystal silicon carbide (0001) surface in sliding contact with various metals. Sliding direction, $\langle 10\bar{1}0 \rangle$; sliding velocity, 3 millimeters per minute; temperature, 25°C ; vacuum pressure, 10^{-8} pascal.

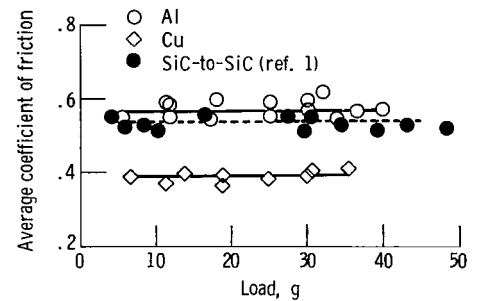


Figure 4. - Average coefficient of friction calculated from maximum peak-heights in friction trace as function of load for aluminum and copper sliding on single-crystal silicon carbide (0001) surface. Single pass of metal rider; sliding direction, $\langle 10\bar{1}0 \rangle$; sliding velocity, 3 millimeters per minute; temperature, 25°C ; vacuum pressure, 10^{-8} pascal.

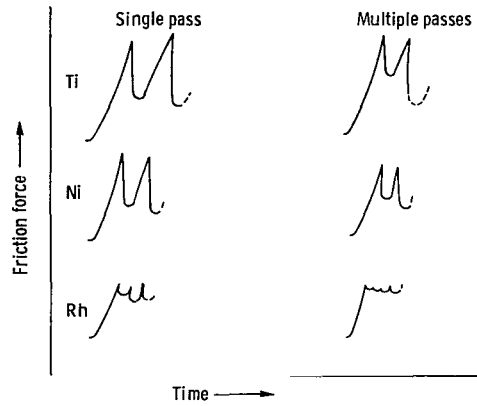


Figure 5. - Friction traces for titanium, nickel, and rhodium sliding on single-crystal silicon carbide (0001) surface. Sliding direction, $\langle 10\bar{1}0 \rangle$; sliding velocity, 3 millimeters per minute; temperature, 25°C ; vacuum pressure, 10^{-8} pascal.

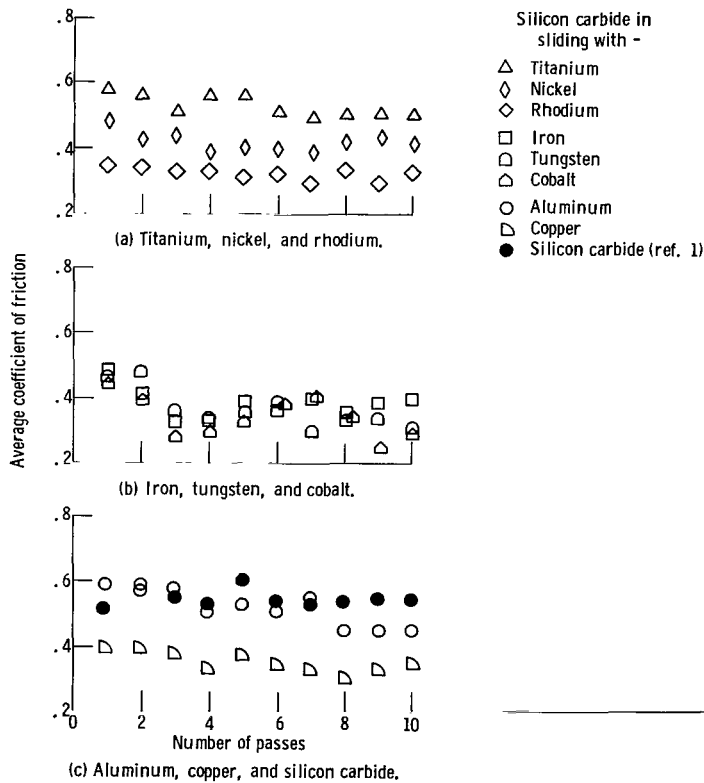
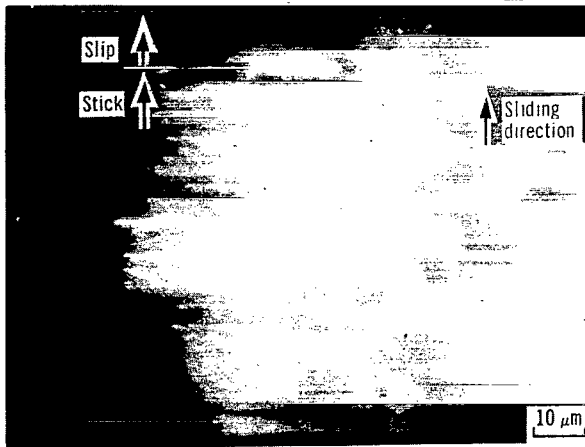
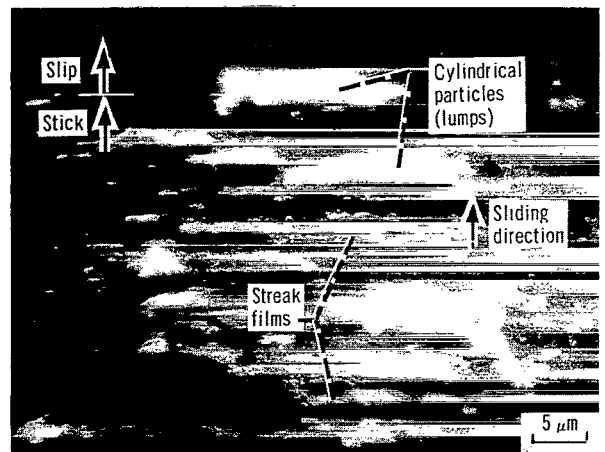


Figure 6. - Average coefficient of friction, calculated from maximum-peak-heights in friction trace, as function of number of passes of metal rider across single-crystal silicon carbide (0001) surface in vacuum. Sliding direction, $\langle 10\bar{1}0 \rangle$; sliding velocity, 3 millimeters per minute; load, 30 grams; temperature, 25°C ; vacuum pressure, 10^{-8} pascal.



(b) Aluminum K_{α} X-ray map; 1.5×10^4 counts.



(c) Scanning electron micrograph (high magnification).

Figure 7. - Aluminum transferred to single-crystal silicon carbide at commencement of sliding as a result of single pass of rider in vacuum. Silicon carbide (0001) surface; sliding direction $\langle 10\bar{1}0 \rangle$; sliding velocity, 3 millimeters per minute; load, 30 grams; temperature, 25° C; vacuum pressure, 10^{-8} pascal.

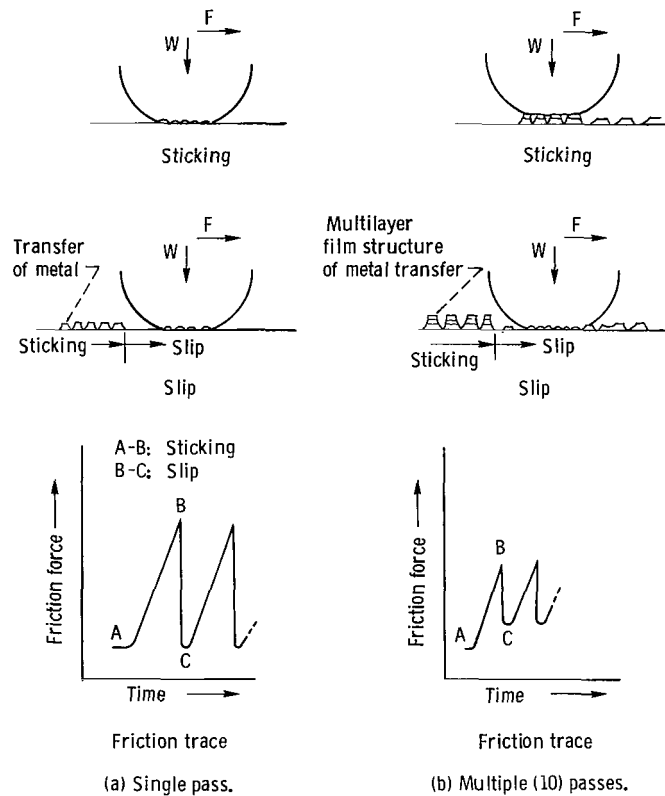
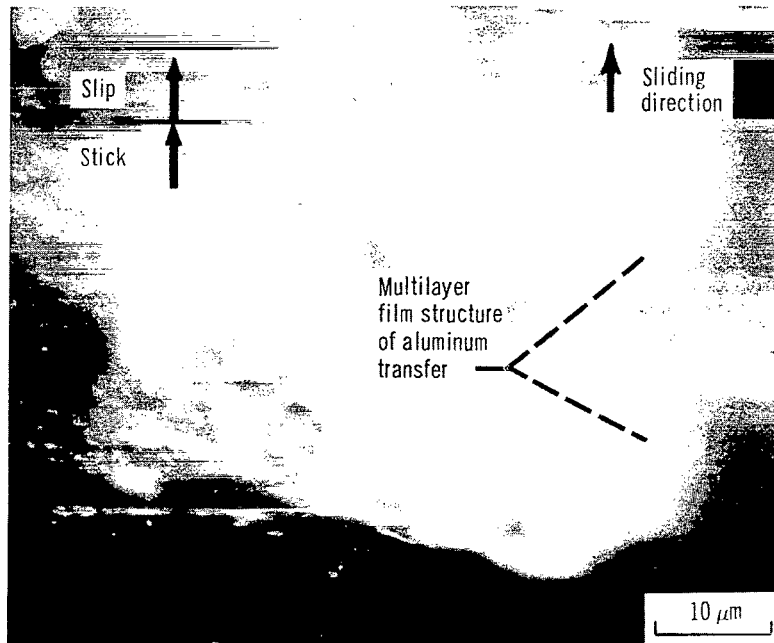
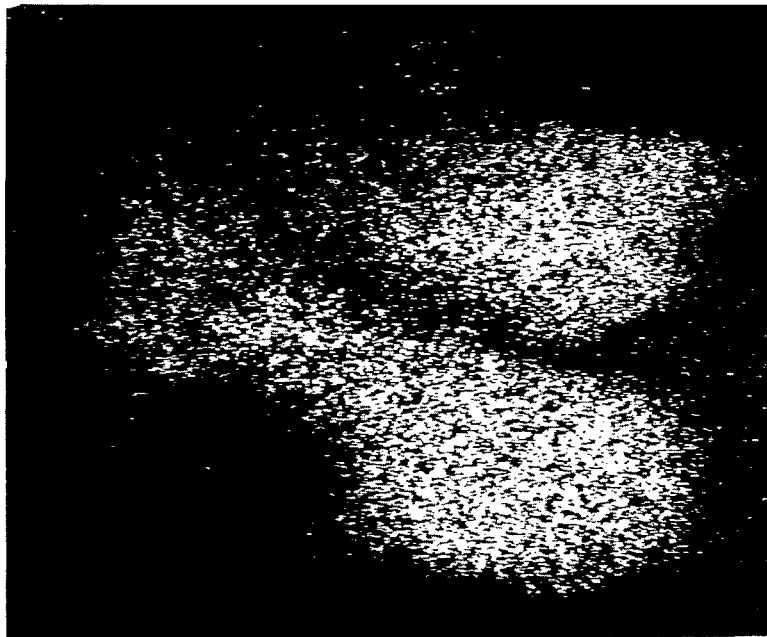


Figure 8. - Intermittent motion of friction and schematic model of metal transfer. Single and multiple passes of aluminum rider on single-crystal silicon carbide (0001) surface; sliding direction, $\langle 10\bar{1}0 \rangle$; sliding velocity, 3 millimeters per minute; load, 30 grams; temperature, 25° C; vacuum pressure, 10^{-8} pascal.



(a) Scanning electron micrograph.



(b) Aluminum $K\alpha$ X-ray map; 1.5×10^4 counts.

Figure 9. - Aluminum transferred to single-crystal silicon carbide at commencement of sliding as a result of multiple passes of rider in vacuum. Wear track on silicon carbide (0001) surface; sliding direction, $\langle 10\bar{1}0 \rangle$; sliding velocity, 3 millimeters per minute; load, 30 grams; temperature, 25° C; vacuum pressure, 10^{-8} pascal.

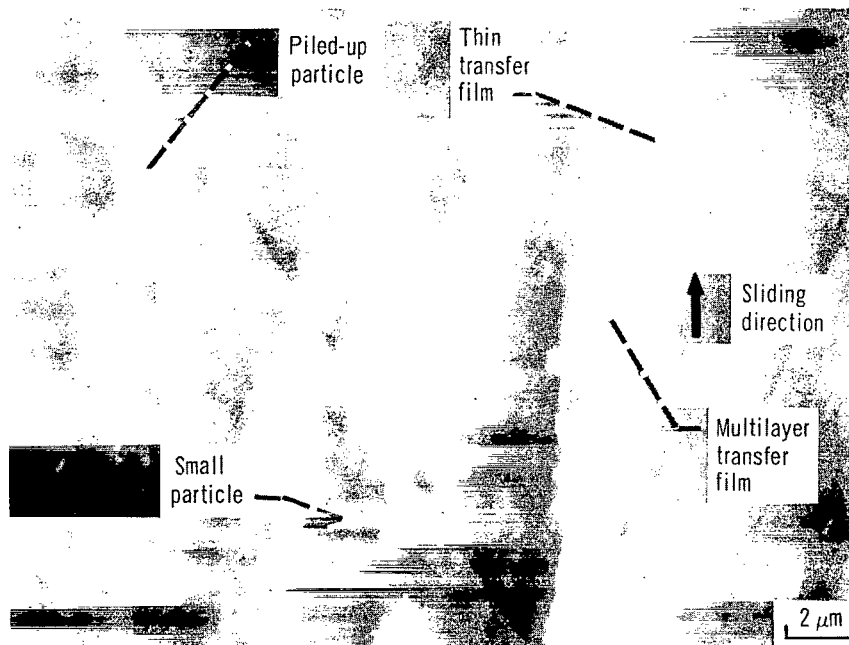
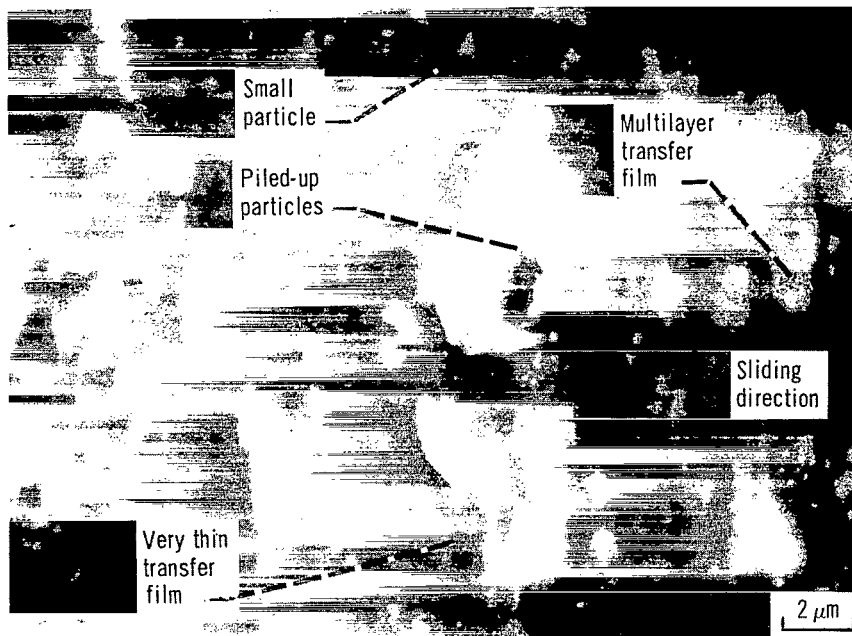


Figure 10. - Aluminum transferred to single-crystal silicon carbide during sliding as a result of multiple passes of rider in vacuum. Scanning electron micrographs of a wear track on silicon carbide (0001) surface during sliding. Sliding direction, $\langle 10\bar{1}0 \rangle$; sliding velocity, 3 millimeters per minute; load, 30 grams; temperature, 25° C; vacuum pressure, 10^{-8} pascal.

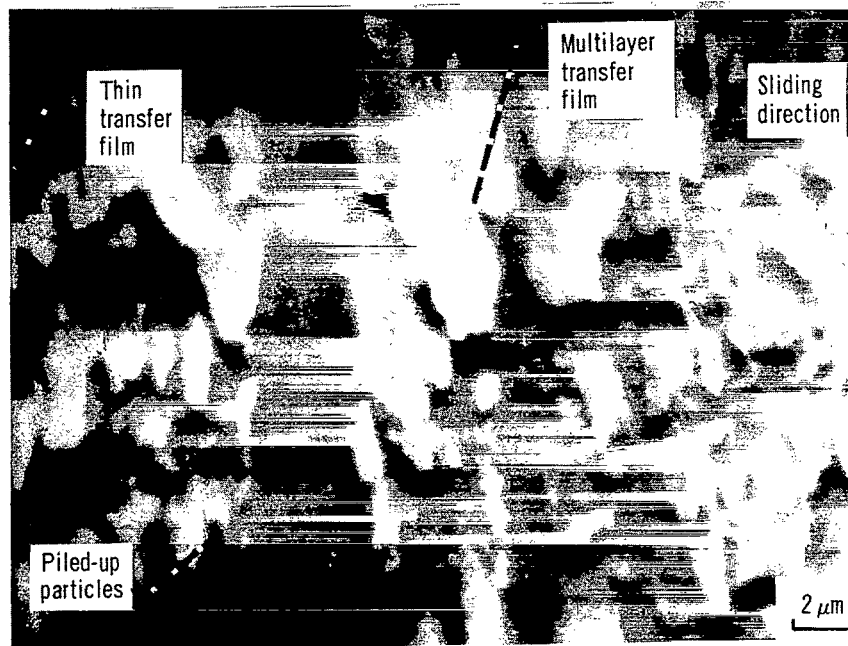
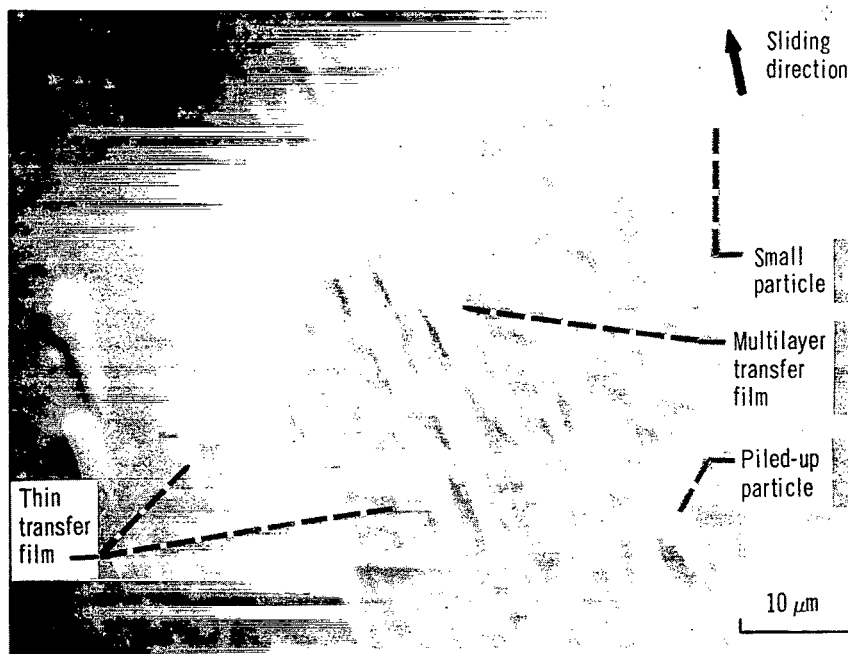


Figure 11. - Titanium transferred to single-crystal silicon carbide during sliding as a result of multiple passes of rider in vacuum. Scanning electron micrographs of a wear track on silicon carbide (0001) surface during sliding. Sliding direction, $\langle 10\bar{1}0 \rangle$; sliding velocity, 3 millimeters per minute; load, 30 grams; temperature, 25°C; vacuum pressure, 10^{-8} pascal.

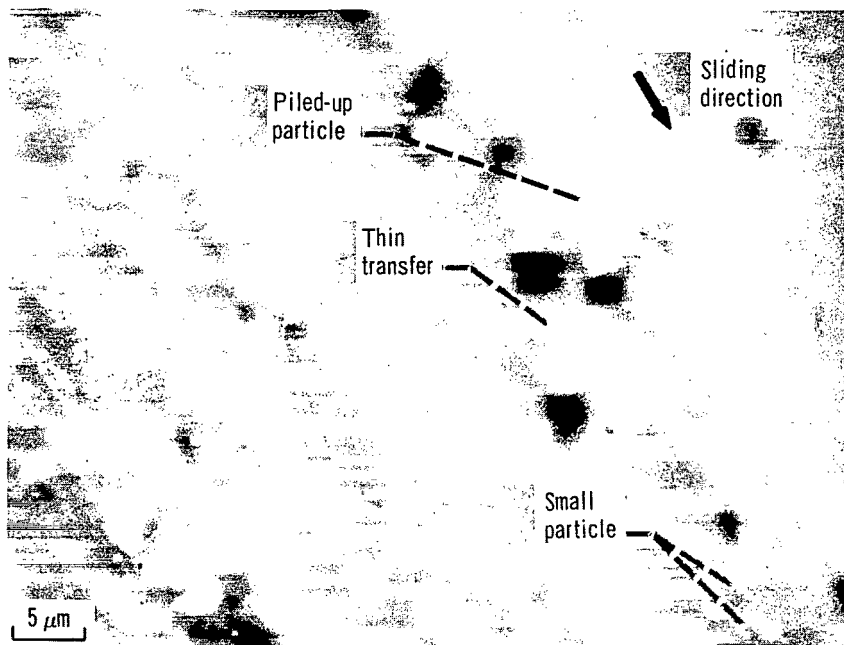
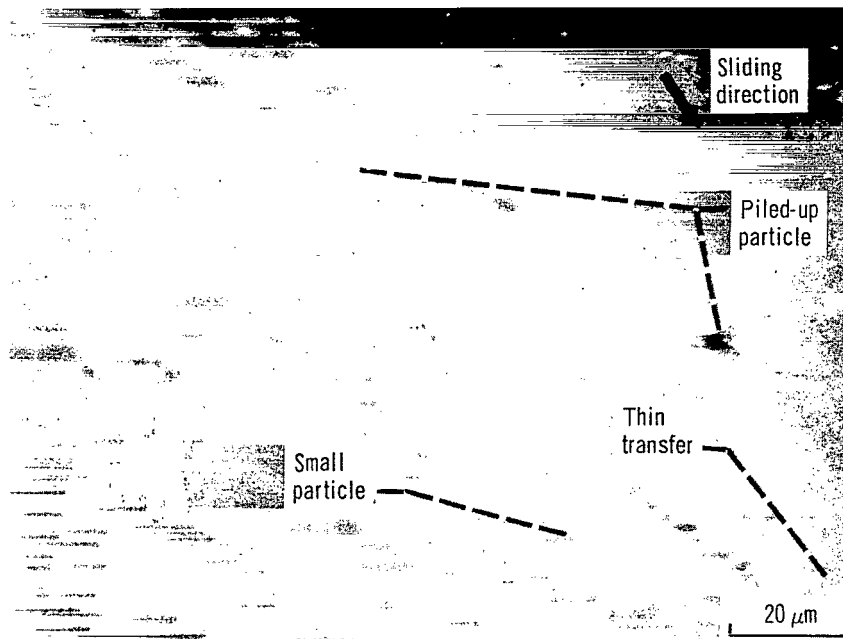


Figure 12. - Nickel transferred to single-crystal silicon carbide as a result of multiple passes of rider in vacuum. Scanning electron micrographs of a wear track on silicon carbide (0001) surface during gross sliding. Sliding direction, $\langle 10\bar{1}0 \rangle$; sliding velocity, 3 millimeters per minute; load, 30 grams; temperature, 25°C; vacuum pressure, 10^{-8} pascal.

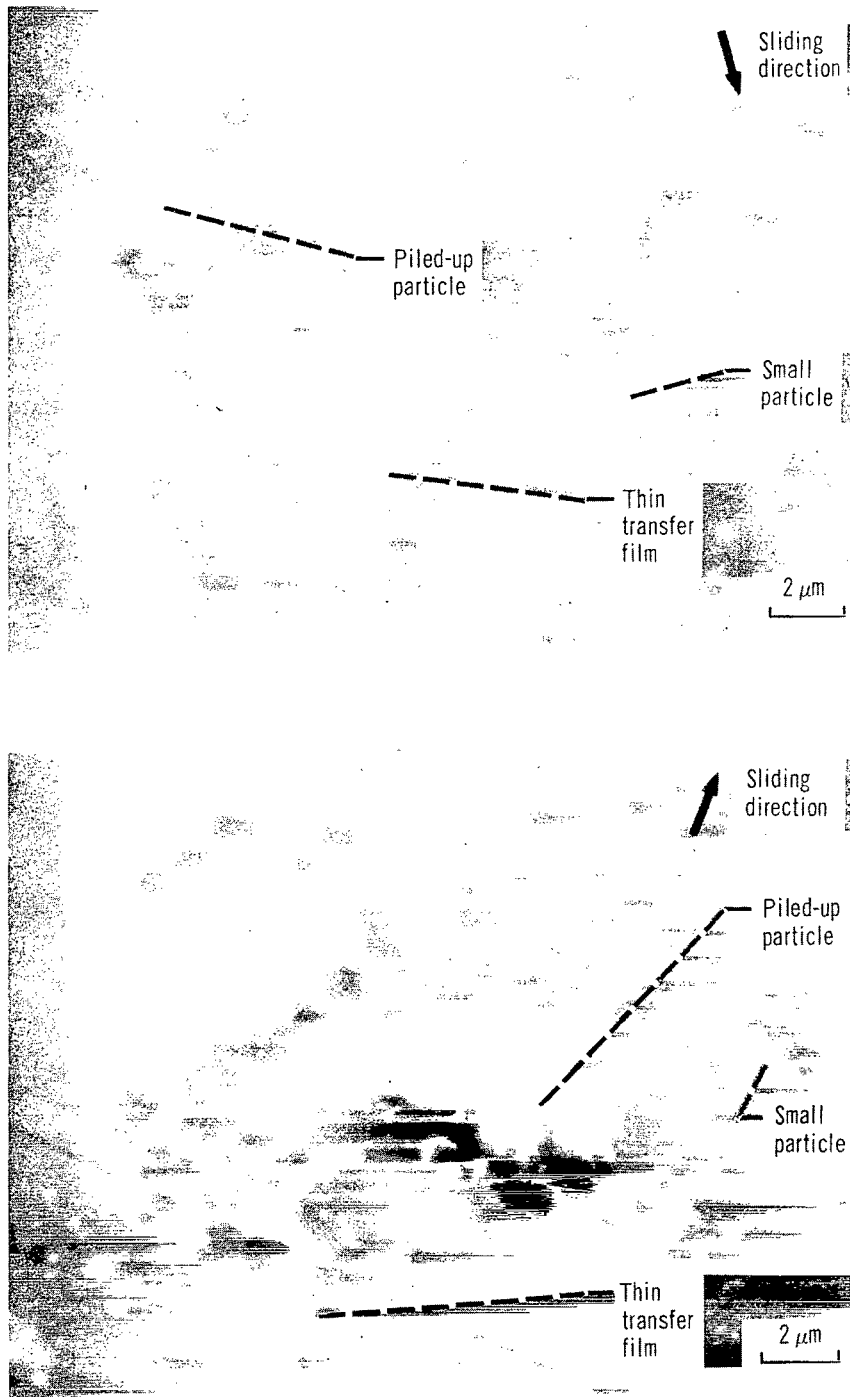


Figure 13. - Copper transferred to single-crystal silicon carbide as a result of multiple passes of rider in vacuum. Scanning electron micrographs of a wear track on silicon carbide (0001) surface during gross sliding. Sliding direction, $\langle 10\bar{1}0 \rangle$; sliding velocity, 3 millimeters per minute; load, 30 grams; temperature, 25° C; vacuum pressure, 10^{-8} pascal.

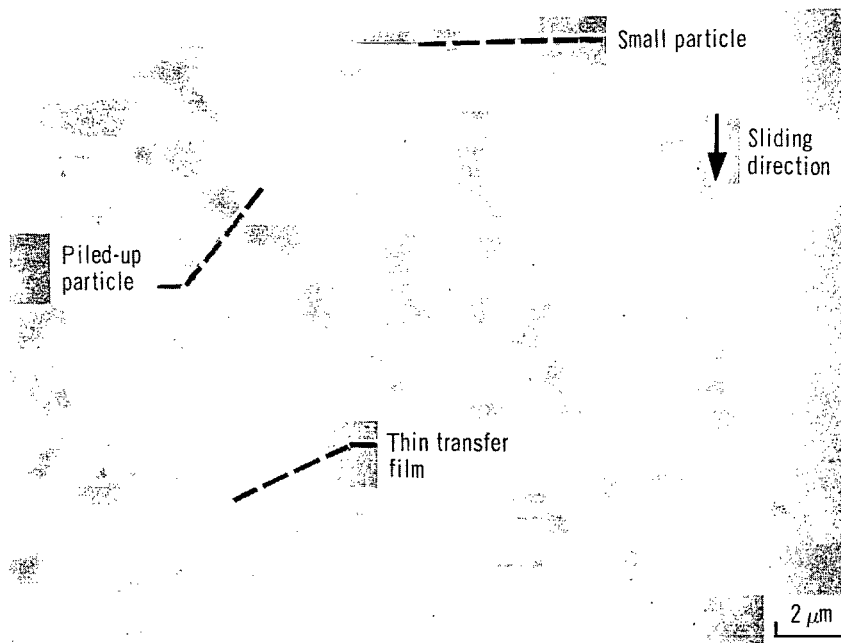
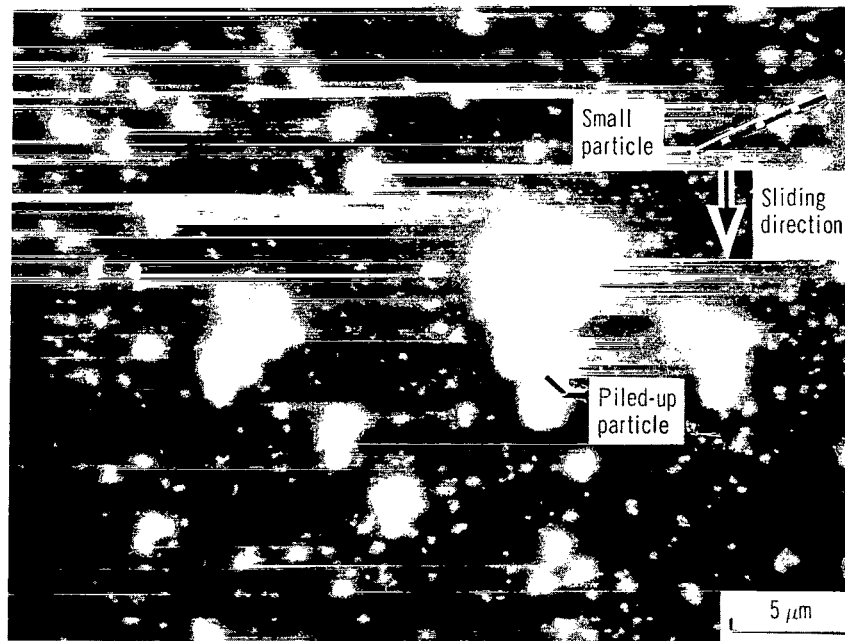


Figure 14. - Cobalt transferred to single-crystal silicon carbide as a result of multiple passes of rider in vacuum. Scanning electron micrographs of a wear track on silicon carbide (0001) surface during gross sliding. Sliding direction, $\langle 10\bar{1}0 \rangle$; sliding velocity, 3 millimeters per minute; load, 30 grams; temperature, 25° C; vacuum pressure, 10^{-8} pascal.

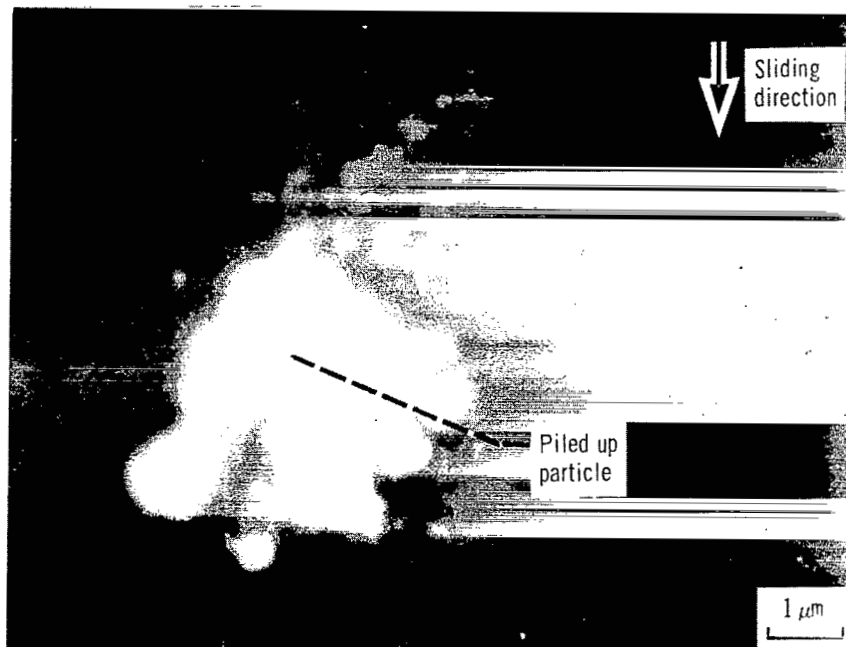
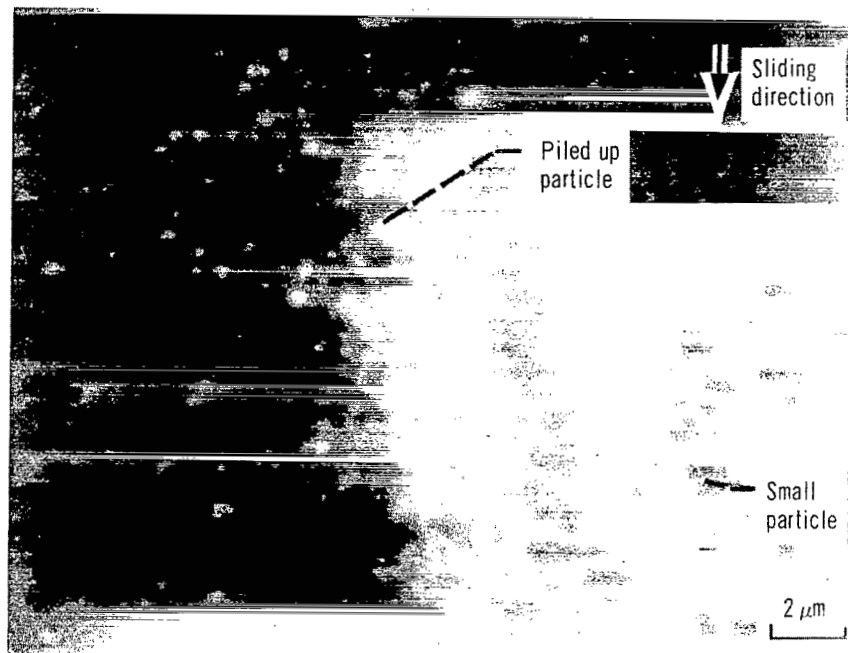
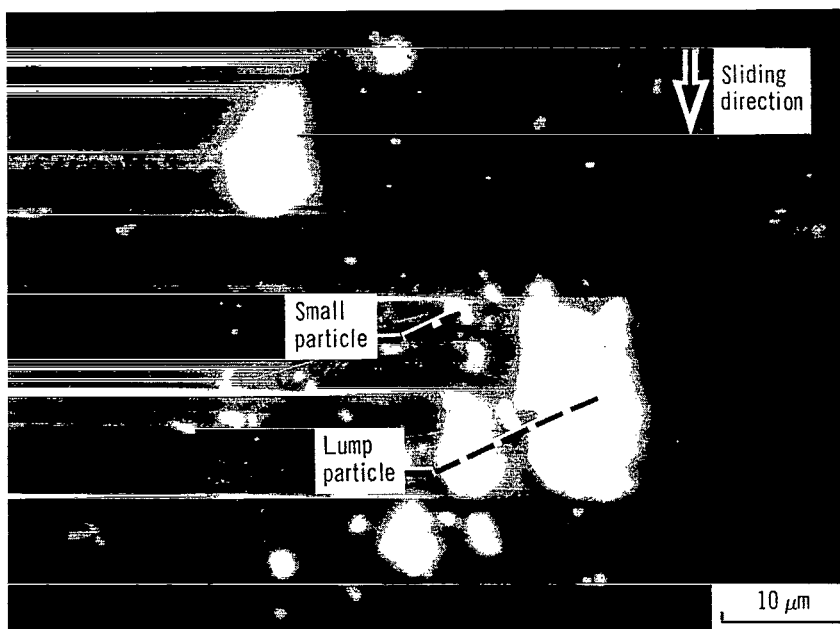
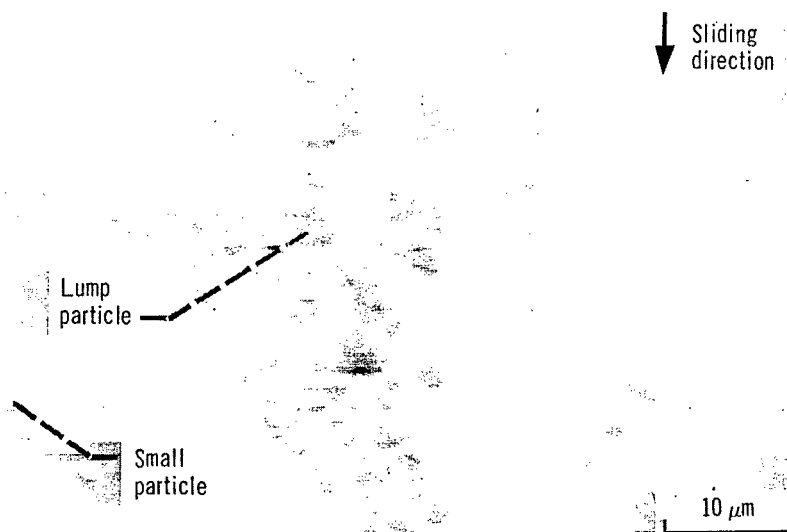


Figure 15. - Iron transferred to single-crystal silicon carbide as a result of multiple passes of rider in vacuum. Scanning electron micrographs of wear track on silicon carbide (0001) surface during sliding. Sliding direction, $\langle 10\bar{1}0 \rangle$; sliding velocity, 3 millimeters per minute; load, 30 grams; temperature, 25° C; vacuum pressure, 10^{-8} pascal.



Single-pass.



Ten passes over the same track.

Figure 16. - Tungsten transferred to single-crystal silicon carbide as results of single and multiple passes of rider in vacuum. Scanning electron micrographs of wear tracks on silicon carbide (0001) surface during gross sliding. Sliding direction, $\langle 10\bar{1}0 \rangle$; sliding velocity, 3 millimeters per minute; load, 30 grams; temperature, 25° C; vacuum pressure, 10^{-8} pascal.

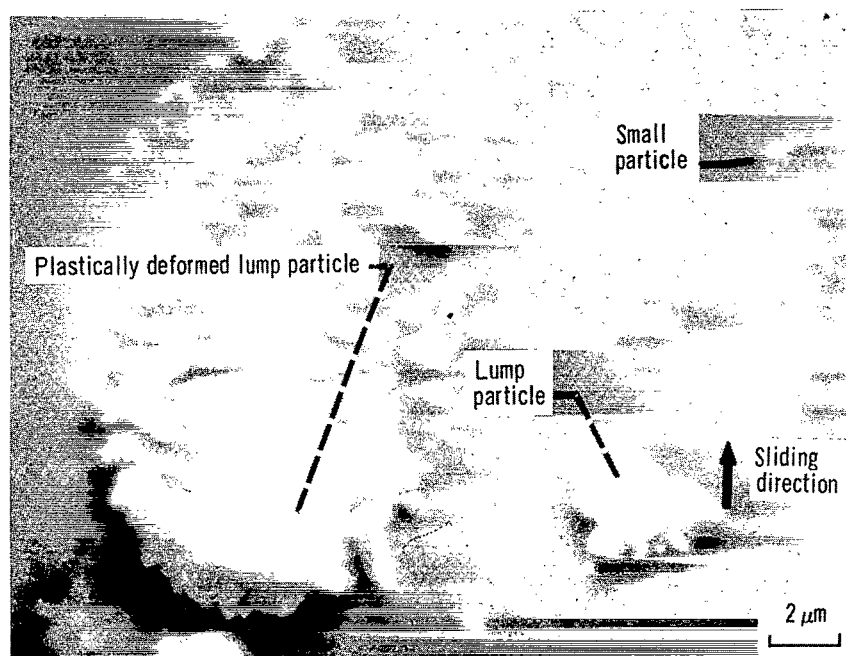
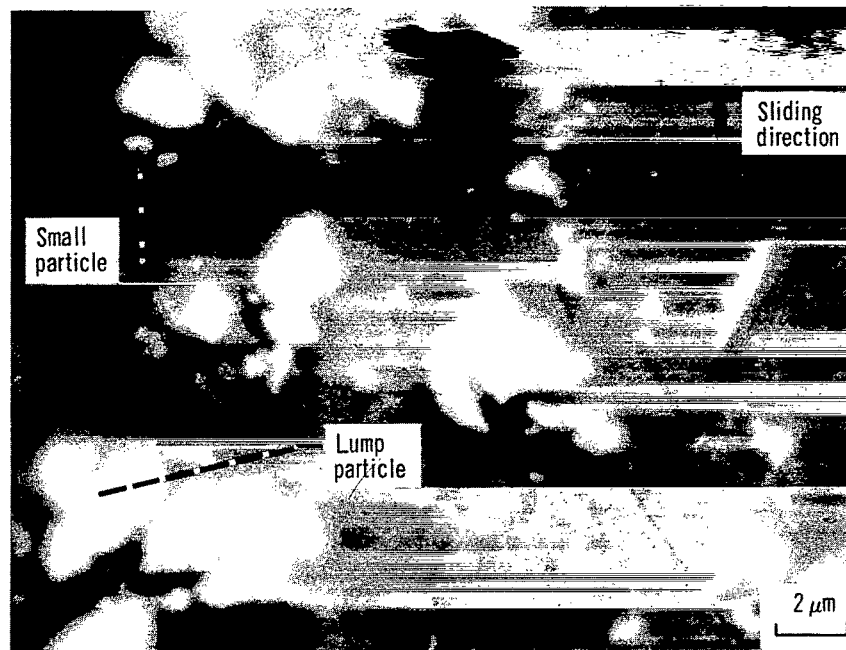


Figure 17. - Rhodium transferred to single-crystal silicon carbide as results of multiple passes of rider in vacuum. Scanning electron micrographs of wear track on silicon carbide (0001) surface during sliding. Sliding direction, $\langle 10\bar{1}0 \rangle$; sliding velocity, 3 millimeters per minute; load, 30 grams; temperature, 25°C; vacuum pressure, 10^{-8} pascal.

| | | | | | |
|---|--|---|--|---|--|
| 1. Report No. NASA TP-1191 | | 2. Government Accession No. | | 3. Recipient's Catalog No. | |
| 4. Title and Subtitle FRICITION AND METAL TRANSFER FOR SINGLE-CRYSTAL SILICON CARBIDE IN CONTACT WITH VARIOUS METALS IN VACUUM | | | | 5. Report Date April 1978 | |
| | | | | 6. Performing Organization Code | |
| 7. Author(s) Kazuhisa Miyoshi and Donald H. Buckley | | | | 8. Performing Organization Report No. E-9307 | |
| 9. Performing Organization Name and Address National Aeronautics and Space Administration Lewis Research Center Cleveland, Ohio 44135 | | | | 10. Work Unit No. 506-16 | |
| | | | | 11. Contract or Grant No. | |
| 12. Sponsoring Agency Name and Address National Aeronautics and Space Administration Washington, D.C. 20546 | | | | 13. Type of Report and Period Covered Technical Paper | |
| | | | | 14. Sponsoring Agency Code | |
| 15. Supplementary Notes | | | | | |
| 16. Abstract <p>Sliding friction experiments were conducted with single-crystal silicon carbide in contact with transition metals (tungsten, iron, rhodium, nickel, titanium, and cobalt), copper, and aluminum. Results indicate the coefficient of friction for a silicon carbide-metal system is related to the bond character and relative chemical activity of the metal. The more active the metal, the higher the coefficient of friction. All the metals examined transferred to the surface of silicon carbide in sliding. The chemical activity of metal to silicon and carbon and shear modulus of the metal may play important roles in metal transfer and the form of the wear debris. The less active and greater resistance to shear the metal has, with the exception of rhodium and tungsten, the less transfer to silicon carbide.</p> | | | | | |
| 17. Key Words (Suggested by Author(s)) Single-crystal silicon carbide; Friction; Metal transfer; Chemical activity; Shear modulus | | | 18. Distribution Statement Unclassified - unlimited STAR Category 27 | | |
| 19. Security Classif. (of this report) Unclassified | | 20. Security Classif. (of this page) Unclassified | | 21. No. of Pages 25 | |
| | | | | 22. Price* A02 | |

* For sale by the National Technical Information Service, Springfield, Virginia 22161

National Aeronautics and
Space Administration

Washington, D.C.
20546

Official Business

Penalty for Private Use, \$300

THIRD-CLASS BULK RATE

Postage and Fees Paid
National Aeronautics and
Space Administration
NASA-451



13 1 10, C, 040878 S00903DS
DEPT OF THE AIR FORCE
AF WEAPONS LABORATORY
ATTN: TECHNICAL LIBRARY (SUL)
KIRTLAND AFB NM 87117

NASA

POSTMASTER:

If Undeliverable (Section 158
Postal Manual) Do Not Return